INVESTIGATION OF THE INCORPORATION OF ZIRCONIUM INTO THE HYDROXYAPATITE STRUCTURE OF ZIRCONIA-HYDROXYAPATITE COMPOSITES AND ZIRCONIUM HYDROXYAPATITE POWDERS

Lameiras, Fernando Soares
CDTN – Centro de Desenvolvimento da Tecnologia Nuclear, R. Professor Mário Werneck, s/n, Caixa Postal 941, Cidade Universitária, Pampulha, Belo Horizonte, MG, CEP 30123-970, Brazil

Barrea, Raul Alberto
LNLS – Laboratório Nacional de Luz Síncrotron, Caixa Postal 6192, Campinas, SP, Brazil, CEP 13084-971.
Universidad Nacional de Córdoba/Facultad de Matemática, Astronomia y Física, 5010, Córdoba, Argentine.

Silva, Viviane Viana
CDTN – Centro de Desenvolvimento da Tecnologia Nuclear, R. Professor Mário Werneck, s/n, Caixa Postal 941, Cidade Universitária, Pampulha, Belo Horizonte, MG, CEP 30123-970, Brazil
UninCor – Universidade Vale do Rio Verde, Av. Castelo Branco, 82, Chácara das Rosas, Três Corações, MG, CEP 37410-000, Brazil
vvs@cdtn.br

Andrade, Leandro Hostalácio Freire de Andrade
CDTN – Centro de Desenvolvimento da Tecnologia Nuclear, R. Professor Mário Werneck, s/n, Caixa Postal 941, Cidade Universitária, Pampulha, Belo Horizonte, MG, CEP 30123-970, Brazil

Macedo, Waldemar Augusto de Almeida
CDTN – Centro de Desenvolvimento da Tecnologia Nuclear, R. Professor Mário Werneck, s/n, Caixa Postal 941, Cidade Universitária, Pampulha, Belo Horizonte, MG, CEP 30123-970, Brazil

Abstract. *This study aims to investigate the probable mechanisms of isomorphous substitution of Ca^{2+} by Zr^{4+} ions in the hydroxyapatite crystal structure of zirconia-hydroxyapatite composites (ZH) and zirconium hydroxyapatite (ZrHA powders based on their ability to undergo a series of cationic substitutions related to size proximity of the ions involved and the local neutrality of the crystal structure. X-ray diffraction (XRD) was used to characterize the powders and to determine lattice parameter dimensions (a-axis and c-axis); energy dispersive spectroscopy (EDS) was used to perform zirconium elemental analysis, extended X-ray absorption fine structure spectroscopy (EXAFS) to provide information about the local environment of zirconium and calcium atoms in the hydroxyapatite phase, and X-ray photoelectron spectroscopy (XPS) to investigate the presence of zirconium on the surface of hydroxyapatite phase particles. The results obtained suggest that zirconium ions may be incorporated into the hydroxyapatite structure of both zirconium hydroxyapatite and zirconia-hydroxyapatite composite powders by different mechanisms.*

Keywords: *zirconia-hydroxyapatite, isomorphous substitution, EXAFS (X-ray absorption fine structure spectroscopy), XPS (X-ray photoelectron spectroscopy)*

1. Introduction

Calcium hydroxyapatite (HA_p), $Ca_{10}(PO_4)_6(OH)_2$, a double salt of tricalcium phosphate and calcium hydroxide, is a member of a large family of isomorphous substances and the main inorganic component of hard tissues of living being systems (LeGeros and LeGeros, 1991; Ravaglioli and Krajewski, 1992; Poster, Betts and Blumenthal, 1980). Being an area of intensive interdisciplinary research, the study of HA_p has experienced rapid strides in the recent years by providing a comprehensive review and updating information on its principal aspects, such as formation conditions, synthesis techniques, characterization, heteroionic isomorphous substitutions leading to the formation of solid solutions and composites, its hole in the incorporation of toxic ions in human skeletal and dental systems, and from the biological viewpoint, on its solubility equilibrium (Narasaraju, 1996; LeGeros, 1991; Tas *et al.*,1997; Silva and Fernandes, 1997; Silva, Lameiras and Lobato, 2002). Although synthetic hydroxyapatite exhibits low fracture toughness , improvement of mechanical properties can be achieved by the incorporation of a resistant oxide phase into its structure without affecting its biocompatibility (Silva, Lameiras and Lobato, 2002), such as zirconia partially stabilized by calcia (Takaqi, *et al.*,1992; Chang *et al.*,1997; Silva, Lameiras and Domingue, 2001). Co-precipitation processes of precursor reagent solutions are suitable to synthesize zirconia-hydroxyapatite composites (Silva and Lameiras, 2000; Silva, Lameiras and

Domingues, 2003) as they yield more homogeneous dispersions. This approach allows controlling the decomposition of hydroxyapatite because of the lower sintering temperatures achieved.

A characteristic property of HA_p is its ability to incorporate a series of cations (Narasaraju, 1996; LeGeros, 1991; Samachson and Schmitz, 1969) and anions (Narasaraju, 1996; LeGeros, 1991; Nadal *et al.*, 1970; Neuman, Toribara and Mulryan, 1956; Elliot, Holcomb and Young, 1985) into its crystal lattice, which is influenced by charge similarity and ions size proximity according to an isomorphous substitution mechanism. In a previous study proposed by Silva and Lameiras (2000), it was suggested an isomorphous substitution mechanism of Ca^{2+} by Zr^{4+} ions in the crystal structure of the hydroxyapatite (HA) phase in two kinds of ZH powders (Z4H6 and Z6H4) as a consequence of a possible decalcification of this phase followed by the incorporation of one Zr^{4+} ion from the zirconia phase into intermediate sites located between two Ca^{2+} ions which leave the lattice. However, this proposition should be substantiated by experimental investigation involving the local environment of zirconium and calcium atoms in the crystal lattice of the hydroxyapatite phase as well as the characterization of the surface of the particles of this phase.

The present study is intended to investigate the mechanism proposed to explain the incorporation of zirconium ions in the HA structure for both ZH powders. ZrHA powders with similar zirconium content in the HA phase were also evaluated for comparison. This investigation was carried out using EXAFS and XPS techniques, in addition to XRD and EDS as complementary measurements.

2. Materials and Methods

2.1. Powder synthesis

Two fine nanocrystalline ZH powders, Z4H6 (41.2 nm) and Z6H4 (31.8 nm) with 40 and 60 vol% of zirconia partially stabilized by 5 mol % CaO (ZO) content respectively, were previously prepared by co-precipitation method (Silva, Lameiras and Domingues, 2003). The complementary phase is HA. The phases of the composites are symbolized by Z for the ZO phase and H for the HA phase. XRD patterns of the both ZH powders (Silva and Lameiras, 2000) reveal the presence of peaks corresponding to monoclinic zirconia (m-ZrO_2), tetragonal zirconia (t-ZrO_2) and calcium zirconium oxide $Ca_{0.15}Zr_{0.85}O_{1.85}$ phases, as well as $Ca_{10}(PO_4)_6(OH)_2$ peaks separately.

Zirconium hydroxyapatite (ZrHA) powders were also synthesized through mixing aqueous solutions of $Ca(NO_3)_2$ 1.0 M and $(NH_4)_2HPO_4$ 0.6 M, and an acid aqueous solution of $ZrO(NO_3)_2$ in the presence of NH_4OH under vigorous agitation for 7 h followed by a resting period of 17 h at room temperature and pH > 10. The resulting precipitate was dispersed and filtrated under vacuum, first in hot water, then in acetone, and finally in petroleum ether. Next, the material was dried and calcined at 800 °C for 3 h in air. Two different powders were obtained: Zr5HA95 and Zr10HA90 with 5.0 and 10 wt. % of zirconium content, respectively. Each one was used for comparison with the composite with similar zirconium content in the HA phase. XRD patterns (not presented here) revealed that both powders are single phase.

Powders of pure ZO (Silva and Domingues, 1997) and HA (Silva and Fernandes, 1997) phases were taken as EXAFS and XPS standards for zirconium and calcium measurements, respectively.

2.2. Characterization techniques

Standard XRD (Rigaku θ-2θ diffractometer using nickel-filtered CuK_α radiation) was used to determine a-axis and b-axis lattice parameter dimensions.

Zirconium elemental analysis was performed by EDS measurements (Jeol JMC-35C microprobe).

Information on the local environment of zirconium and calcium atoms in the HA phase was provided by EXAFS spectra. They were recorded at the synchrotron radiation source of LNLS at Ca and Zr K-edges using FRX beam line running at 1.8-2.0 GeV and 60-100 mA. Double crystal channel-cut Si (111) and Si (220) monochromators were used for Ca and Zr monochromatic source calibration, respectively. Transmittance was measured for each position of the monochromator corresponding to a photon energy of 3.95-5.00 keV for Ca and 17-19 keV for Zr. Powder samples were layered on a polymeric membrane after filtration with acetone and supported by strips of sellotape. Data were analyzed based on approximation to the spherical-electron theory (Lee and Petry, 1975) using WinXAS code (Ressler, 1997).

Information on the presence of zirconium on the surface of HA phase was extracted from XPS data using a VG CLAM2 spectrometer and non-monochromatic Mg K_α excitation source (hν = 1253 eV). Survey and high-resolution spectra were acquired at pass-energies of 50 eV and 20 eV, respectively. The binding energy scale was calibrated by measuring the reference peak of C *1s* from the contamination of the surface on (BE = 285 eV). A least- square peak fitting routine was used for the analysis of XPS spectra to separate elemental species in different valence states.

3. Results and discussion

3.1. XRD and EDS analysis

Table 1 lists a-axis and c-axis lattice parameters and zirconium content data for Z4H6, Z6H4, Zr5HA95, and Zr10HA90 samples, as well as for HA and ZO standards. EDS analysis revealed 5 wt % and 10 wt % contents of zirconium in the HA phase of Z6H4 and Z4H6 powders, respectively. Lower values of a-axis and c-axis lattice parameters were found for the HA phase of the Z6H4 composite in comparison to those of HA standard, while higher values were observed for the Z4H6 composite. However, the corresponding c/a ratio for these systems presented no significant variation in comparison to HA standard. This reveals that although EDS results indicate the presence of zirconium in the HA phase in these composites, their crystal structures resemble those of the HA standard. A similar behavior was also observed for the ZO phase for both composites in relation to the ZO standard. This may be an indication of the incorporation of a small fraction of the total number of zirconium atoms from the ZO phase into the original crystal lattice of HA or at HA-ZO interface sites during powder synthesis process, despite significant local lattice distortions into the HA and ZO phases of the Z4H6 and Z6H4 composites are not evidenced.

In contrast, higher values for the c/a ratio were found for the Zr5HA95 and Zr10HA90 powders in comparison to the HA standard. This may be an indication of the incorporation of zirconium ions into the original HA lattice as a result of structural distortions during powder synthesis process.

Table 1. Data of a-axis and c-axis lattice parameters and zirconium content for HA and ZO standards, and Z4H6, Z6H4, Zr5HA95 and Zr10HA90 samples

					Composite			
	Standard		Zirconium hydroxyapatite		**Z6H4**		**Z4H6**	
Sample	HA	ZO	Zr5HA95	Zr10HA90	HA	ZO	HA	ZO
a (Å)	9.431	5.12	9.381	9.408	9.415	5.12	9.443	5.12
c (Å)	6.876	5.15	6.939	6.958	6.858	5.12	6.882	5.13
c/a	0.729	1.01	0.740	0.739	0.728	1.00	0.729	1.00
Zr-content (wt%)	-	72.6	5.00	10.0	5.04	64.0	10.0	40.5

3.2. EXAFS analysis

Figure 1 shows the k-weighed Fourier transform (FT) of the Zr K edge EXAFS for pure ZO (taken as standard for zirconium), Z4H6, and Z6H4 samples. Although the FT curves exhibit similarity for the peaks positions, differences significantly greater are observed for the peak intensities around 3.31 A corresponding to the second zirconium environment (zirconium atoms). This behavior is more marked for the Z4H6 sample richer in zirconium content (10 wt. %). Investigations of EXAFS measurements using nanocrystallite oxides (Li, Chen and Penner-Halm, 1993a and 1993b) suggest this behavior can be associated to a progressive reduction in the zirconium coordination number as a function of the distance. The presence of a large fraction of zirconium atoms at intergrain regions (surfaces or interfaces) may also have contributed for the reduction of the Zr-Zr coordination number. As surfaces or interfaces in nanocrystallite materials can be considered as amorphous regions with a range of radial distances (Gleiter, 1992), it could attenuate the EXAFS signal and consequently reduce peak amplitudes in the Fourier transform resulting in reduced coordination numbers. On the other hand, these regions are similar to the grain boundaries and are not highly disordered (Stern, 1995). Here the Zr-Zr coordination number may be reduced if a fraction of the total number of zirconium atoms present into the ZO phase is incorporated into the crystal lattice of HA or at HA-ZO interface sites.

Figure 2.a shows the k^3-weighed FT of the Zr K edge EXAFS for ZO, Zr5HA95, and Zr10HA90. The ZO and Zr5HA95 curves present the closest shell environments quite different. The Zr5HA95 curve exhibits peaks at 1.10 Å and 1.56 A, whereas only one peak at 1.60 A is observed in the ZO curve. Although similar environments at 3.35 A are observed for both curves, significant variations in the peak positions around 2.20 and 2.90 A are recorded. The Zr5HA95 curve also shows a peak at 2.65 A which is absent in ZO curve. Peaks of higher intensities are found in the Zr5HA95 curve and can be associated to a higher zirconium coordination number. The variations in the peak amplitudes and positions in the ZrHA curves become more significant as the zirconium content in the sample increases. This behavior may be explained in terms of the high levels of point defects (vacancies or impurities) present in the bulk or at the surface of nanocrystallite materials (Allnatt, 1964; Maier, 1995), which affect the coordination number and the radial distance. While simple peaks at 1.10, 1.56 and 2.15 A are observed in the Zr5HA95 curve relative to the three first zirconium environments, respectively, the Zr10HA90 curve exhibits three pairs of peaks (doublets) at 0.92 and 1.27 A, at 1.56 and 2.35 A, and at 2.10 and 2.35 A for the same neighborhoods as a result of the split of each simple peak in a doublet. The three doublets observed in the EXAFS Zr10HA90 curve may be related to of zirconium atoms

incorporated as impurities in the bulk, or at the surface of hydroxyapatite crystallites occupying two different kind of sites in the Zr10HA90 structure.

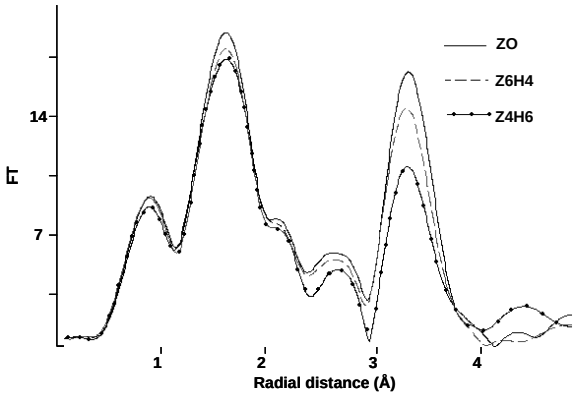

Figure 1. k-weighed Fourier transform (FT) of the Zr K edge EXAFS for pure ZO, Z4H6 and Z6H4 samples.

k^3-weighed FT curves of the Ca K edge EXAFS for pure HA, taken as standard for hydroxyapatite, Zr5HA95, and Zr10HA90 are shown in Figure 2.b. The peaks positioned around 1.90 A suggest a similar environment for calcium atoms for the ZrHA powders in relation to the HA standard. However, different behaviors are observed for others neighborhoods. While the Z5HA95 curve exhibits EXAFS well-defined peaks at 1.0, 1.42, 3.06 , and 3.63 A, peaks poorly resolved relative to the last two environments are observed in the Zr10HA90 curve. In addition, the Zr10HA90 curve presents none peak positioned at radial distances below 1.90 A. This effect is also evidenced around 1.4 A for the HA curve. The peaks at 3.1 and 3.7 A showed in the HA curve are slightly dislocated in relation to the correspondent ones for the Zr5HA95 curve too. However, this behavior is markedly attenuated for the Z4H6 and Z6H4 composite samples, and it may be clearly visualized in k^3-weighed FT curves of Ca K edge EXAFS are shown in Fig. 3.a and 3.b for the pairs curves of Zr5HA95-Z6H4 (with 5 wt.% in Zr) and Zr10HA90-Z4H6 (with 10 wt.% in Zr), respectively. It is important to observe that the samples with lower zirconium content (Fig.3.a) exhibit peaks clearly better resolved, mainly for calcium neighbors (around 3.6 A and 3.8 A for Zr5HA95 and Z6H4, respectively). Otherwise the EXAFS peaks relative to phosphorous neighbors presented worse resolution as evidenced in the FT curves of composite powders (around 3.05 and 3.10 A for Z6H4 and Z4H6, respectively)

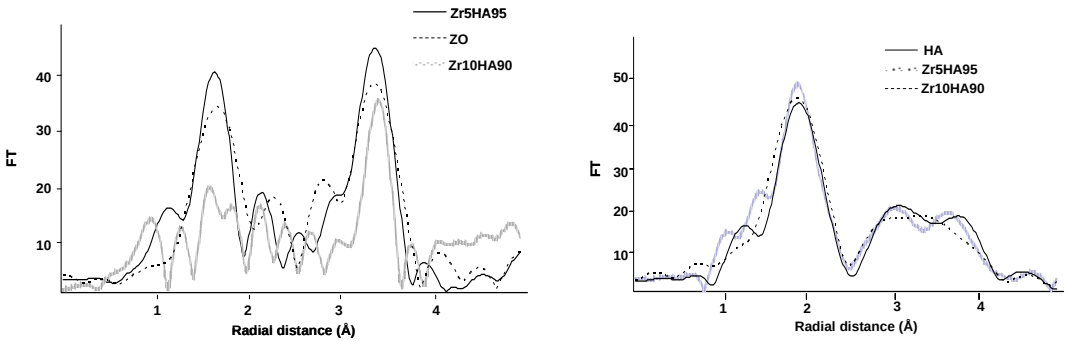

(a) (b)

Figure 2. k^3-weighed Fourier transform (FT) of: (a) the Zr K edge EXAFS for pure ZO, Zr5HA95 and Zr10HA90 samples; (b) the Ca K edge EXAFS for pure HA, Zr5HA95 and Zr10HA90 samples.

3.3. XPS analysis

XPS Ca2p spectra for the HA standard, ZH, and ZrHA samples are shown in Fig. 4.a (HA, Z6H4, and Zr5HA95) and Fig. 4.b (HA, Z4H6 and Zr10HA90). Figure 5 also presents the XPS $P2p_{3/2}$ spectra for all these specimens. A similar doublet with $Ca2p_{3/2}$ and $Ca2p_{1/2}$ typical for Ca^{2+} oxidation state in inorganic calcium-oxygen compounds is evidenced in the XPS spectra for the HA standard and for the ZH specimens. $Ca2p_{3/2}$ binding energies given at XPS

spectra peak position are 347.43 eV, 347.39 eV and 347.30 eV for the HA standard, Z6H4, and Z4H6, respectively, while for the $Ca2p_{1/2}$ binding energies values of 350.98 eV, 350.94 eV and 350.96 eV were found, respectively. The values 133.92 eV, 133.80 eV, and 134.05 eV correspond to the $P2p_{3/2}$ binding energies for the same sequence of the samples. These results are complementary to the EDS and EXAFS analyses since they indicate that the Ca-PO_4^{3-} coordination on the surface of the HA phase present in the ZH samples resembles that of the pure HA standard. This can be an indication that zirconium atoms present in the HA phase are incorporated in its crystal lattice substituting calcium atoms (which can probably have migrated to surface sites) instead of occupying surface sites. This behavior is more evident for the Z4H6 specimen richer in zirconium content.

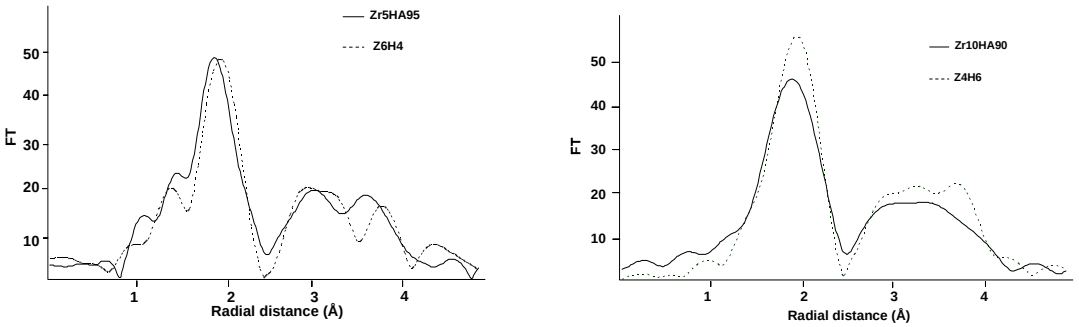

(a) (b)

Figure 3. k^3-weighed Fourier transform (FT) of the Ca K edge EXAFS for (a) Zr5HA95 and Z6H4 samples; (b) Zr10HA90 and Z4H6 samples.

XPS Ca2p spectra for the Zr5HA95 (Fig. 4.a) and Zr10HA90 (Fig. 4.b) samples exhibited lower values for $Ca2p_{3/2}$ and $Ca2p_{1/2}$ binding energies (346.38 eV and 349.92 eV, respectively for Zr5HA95, and 346.76 eV and 350.39 eV, respectively for Zr10HA90). The same behavior was also observed for $P2p_{3/2}$ binding energies (133.05 eV for Zr5HA95, and 133,29 eV for Zr10HA90) as shown in their XPS P2p spectra (Fig. 5). These results suggest that PO_4^{3-} groups can be coordinated with both Ca atoms of HA and Zr atoms, which were deliberately introduced during the synthesis process. Supposedly, the number of Zr^{4+}-PO_4^{3-} bonds increases as a function of the zirconium content in the sample. When PO_4^{3-} is coordinated with Zr^{4+}, the Ca^{2+}-PO_4^{3-} bonds are weakened, while the Zr^{4+}-PO_4^{3-} bonds are strengthened due to the zirconium higher effective charge.

3.4. Isomorphous substitution mechanisms of Ca^{2+} by Zr^{4+} in the HA crystalline structure

Figure 6 shows an approach to the rigid sphere model for the HA phase crystal structure after the incorporation of the Zr^{4+} ions. The OH^- groups are located at the corner of the unit cell. They are surrounded by two groups of three Ca^{2+} ions located within the cell occupying the Ca_{II} positions. Each group describes a triangle. Similarly, O^{2-} ions belonging to the PO_4^{3-} groups also surround OH^- groups. Others six Ca^{2+} ions occupying the Ca_I sites are disposed as a hexagonal arrangement. Zr^{4+} ions are replacing Ca^{2+} ions depending on the position or site occupied in the unit cell.

The results of XRD, EDS, EXAFS, and XPS here obtained for the ZH and ZrHA powders studied provide evidence of the incorporation of Zr^{4+} ions into the HA phase crystalline lattice. This incorporation takes place during the synthesis process since the local charge neutrality and the symmetry of the atomic arrangement in the HA phase original unit cell (taken to be the same as that of HAp) are preserved or not significantly disturbed. Three isomorphous substitution mechanisms are suggested to explain this kind of incorporation: (1) two coplanar and adjacent Ca^{2+} ions occupying Ca_I positions in the unit cell are replaced by one Zr^{4+} ion located equidistantly between both empty adjacent Ca_I positions, here referred to as Zr_I position; (2) two non-coplanar and adjacent Ca^{2+} ions, one of them occupying a Ca_I position and the other a Ca_{II} position in the unit cell, are replaced by one Zr^{4+} ion located equidistantly in an intermediate plane between both empty Ca positions, here referred to as $Zr_{I\text{-}II}$ position. In this case, the Zr^{4+} ion dislocates one O^{2-} ion and thus leads to a higher distortion in the HA phase crystalline lattice; and (3) combination of mechanisms (1) and (2).

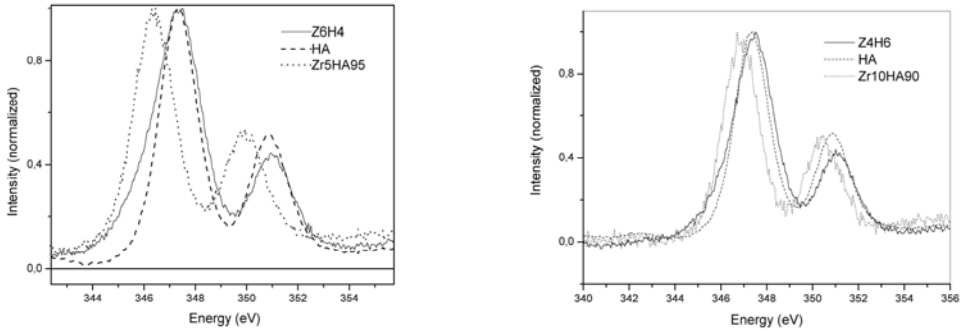

(a) (b)

Figure 4. XPS Ca2p spectra for the (a) HA, Z6H4 and Zr5HA95 samples; (b) HA, Z4H6 and Zr10HA90.

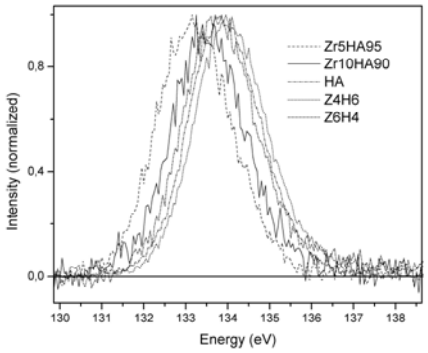

Figure 5. XPS $P2p_{3/2}$ spectra for the HA, Z6H4, Zr5HA95, Z4H6 and Zr10HA90 samples.

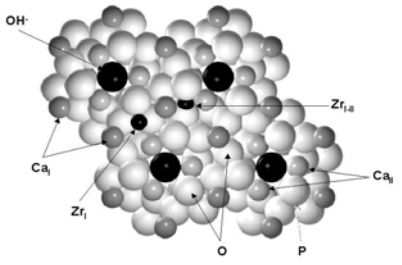

Figure 6. HA phase crystal structure after the incorporation of the Zr^{4+} ions.

Mechanism (1) may explain the incorporation of Zr^{4+} ions into the HA phase structure for ZH powders since similar results were observed for the lattice parameter dimensions (Table 1) and for the local environment of zirconium and calcium atoms in the bulk and at the surface (EXAFS and XPS spectra) for this phase as compared to results of pure HA standard. Low Zr contents present in the HA phase (5 wt.% for Z6H4 and 10 wt.% for Z6H4) may be associated to a higher tendency of Zr^{4+} ions to arrange according to the tetragonal symmetry of the ZO phase (Stevens, 1986) instead of the more complex hexagonal arrangement corresponding to the HA phase (Narasaraju, 1996). The ZO phase has a face-centered CaF_2 structure with each Zr^{4+} ion having symmetry with the oxygen ions, which are arranged in two equal tetrahedra, while the HA crystallizes in hexagonal $P6_{3/m}$ space group. Moreover, the HA phase has the stoichiometric composition of pure HA_p and thus, the number of Ca^{2+} ions present per unit cell correlated with its molecular formula are sufficient to occupy all Ca_I and Ca_{II} positions of its original arrangement. During the synthesis of the composite powders, a few Zr^{4+} ions (from the ZO phase precursor solutions) compete with a much higher number of Ca^{2+} ions per empty positions in the HA phase unit cell, and some of them succeed in being incorporated into the crystalline lattice during the crystallization process. Thus, one Zr^{4+} ion could occupy a Zr_I position located between two coplanar and adjacent Ca_I positions. Although structural distortions may have been created due to the higher effective charge of the Zr^{4+} ion, they are not strong enough to affect the local charge neutrality and the symmetry of the original atomic arrangement in the cell of the HA phase.

Variations recorded for ZrHA powders are significant for the lattice parameters (Table 1) and calcium and zirconium environments (Figs. 2 though 5) and give a strong evidence of a gradual disorder in their atomic arrangement as a function as the zirconium content when Zr^{4+} ions are incorporated into the pure HA unit cell. Such distortions can be explained in terms of the number of Ca_I and Ca_{II} positions per pure HA unit cell, which would not be occupied by Ca^{2+} ions as a consequence of the concentrations of the calcium precursor solutions, deliberately poorer in calcium, used during the synthesis to give the same zirconium content found in the comparative composite (Z6H4 and Zr5HA95 with 5.0 wt. % of zirconium, and Z4H6 and Zr10HA90 with 10 wt. % of zirconium). It means that the Zr^{4+} ions (from the zirconium precursor solution) do not need to compete with the Ca^{2+} ions, whose number is not sufficient to occupy all

Ca_I and Ca_{II} positions of the pure HA original atomic arrangement. At the beginning of the crystallization process, Zr^{4+} ions would tend to migrate preferentially to Zr_I positions located equidistantly between two coplanar and adjacent Ca_I positions (mechanism 1) resulting in smaller distortions in the HA crystalline lattice. Later on, when all the Zr_I positions have been occupied, the remainder Zr^{4+} ions superpose O^{2-} ions while they occupy Zr_{I-II} positions located equidistantly on intermediate planes between one Ca_I position and one Ca_{II} position and thus lead a higher distortion in the atomic arrangement (mechanism 2). For the Zr5HA95 powder, which has a poorer zirconium content, mechanism (1) can be predominating upon mechanism (2) since XRD, EDS, EXAFS and XPS results reveal that the variations observed for the lattice parameters and for the calcium and zirconium environments in the bulk and at the surface of the samples do not alter significantly the original HA crystal structure. However, as the zirconium content increases, more Zr_{I-II} positions can be free and the predominance of mechanism (2) is enhanced for the Zr10HA90 sample, resulting in significantly more marked structural disturb of the HA crystal lattice. This behavior seems to be clearly evidenced by the presence of three pairs of doublets relative to the first three zirconium environments (oxygen atoms belonging to the PO_4^{3-} group) revealed in EXAFS curve shown in Fig. 2a. Each pair of doublet can be associated to Zr_I and Zr_{I-II} positions occupied by Zr^{4+} ions during the HA crystallization process.

4. Conclusions

The local environments of zirconium and calcium atoms in the bulk and on the surface of the hydroxyapatite crystal structure of zirconia-hydroxyapatite composites and zirconium hydroxyapatite powders were investigated using EXAFS and XPS techniques. EDS and XRD complementary measurements were also carried out to evaluate zirconium content and structural distortions in the atomic arrangement in the hydroxyapatite phase. The results obtained indicate different isomorphous substitution mechanisms of Ca^{2+} by Zr^{4+} ions in the hydroxyapatite phase: (1) two coplanar and adjacent Ca^{2+} ions occupying Ca_I positions can be replaced by one Zr^{4+} ion located equidistantly between both empty adjacent Ca_I positions (Zr_I) for the composite powders (Z4H6 and Z6H4); (2) two non-coplanar and adjacent Ca^{2+} ions, one occupying a Ca_I position and the other a Ca_{II} position, can also be replaced by one Zr^{4+} ion located equidistantly on an intermediate plane between both empty Ca positions (Zr_{I-II}) for the zirconium hydroxyapatite powder richer in zirconium content (Zr10HA90). In this case the Zr^{4+} ion dislocates one O^{2-} ion leading to a higher distortion of the hydroxyapatite crystalline lattice; and (3) a combination of the both mechanisms (1) and (2) for the zirconium hydroxyapatite powder poorer in zirconium content (Zr5HA95) so that the higher the zirconium content, the larger the predominance of the mechanism (2) over the mechanism (1).

5. Acknowledgements

The authors express their thanks to CNPq, FAPEMIG and LNLS for financial support. They also gratefully acknowledge the assistance of Walter de Brito (CDTN) and William Tito Soares (UFMG) in XRD and EDS analysis, and Bernardo Salerno Lameiras in the construction of the hydroxyapatite hard sphere model.

6. References

Allnatt, A.R., 1964, "The Concentration of Impurities in the Surface Layers of an Ionic Crystal", J. Phys. Chem, Vol. 68, No. 17, pp. 1763-1768.

Chang, E., Chang, W.J., Wang, B.C. and Yang, C.Y., 1997, "Plasma Spraying of Zirconia - Reinforced Hydroxyapatite Composite Coatings on Titanium", J. Mater. Sci. Mater. Med., Vol. 8, pp. 201-211.

Elliot, J.C., Holcomb, D.W and Young R.A., 1985, "Infrared Determination of the Degree of Substitution of Hydroxyl by Carbonate Ions in Human Dental Enamel", Calcif. Tissue Int., Vol. 37, pp. 372-375.

Gleiter, H., 1992, "Nanostructured Materials", Adv. Mater. (Weinheim, Ger), Vol. 4, pp. 474-481.

LeGeros, R.Z., 1981, "Apatite in Biological Systems", Prog .Cryst. Growth Charact., Vol.4, pp. 1-5.

LeGeros, R.Z., 1991, "Formation and Stability of Synthetic Apatites: Effect of Some Elements", Monographs in Oral Science, Vol. 15, pp. 83-107.

LeGeros, R.Z and LeGeros, J.P., 1991, "Introduction to Bioceramics", Advanced Series in Ceramics., Vol.1, pp. 139-197.

Lee, P.A. and Pendry, J.B., 1975, "Theory of the Extented X-Ray Absorption Fine Structure", Phys. Rer. B, Vol. 11, pp. 2795-2811.

Li, P., Chen, L.W. and Penner-Halm, J.E., 1993a, "X - Ray Absorption Studies of Zirconia Polymorphs: I. Characteristic Local Structures", Phys. Rev. B: Solid State, Vol. 48, No. 14, pp. 10063-10073.

Li, P., Chen, L.W. and Penner-Halm, J.E., 1993b, "X - Ray Absorption Studies of Zirconia Polymorphs: II.Effect of Y_2O_3 Dopant in Zr_2O Structure", Phys. Rev.B: Solid State, Vol. 48, No. 14, pp. 10074-10081.

Maier, J., 1995, "Ionic Conducting in Space Charge Regions", Prog. Solid State Chem., Vol. 23, No. 3, pp. 171-263.

Nadal, M., Trombe, J.C., Bonel, G. and Montel, G., 1970, "Infrared Absorption Spectrometric Study of Some

Substitutions in Carbonated Apatites", J. Schimi, Phy., Vol. 6, pp. 1161-1167.
Narasaraju, T.S.B. and Phebe, D.E., 1996, "Review: Some Physico - Chemical Aspects of Hydroxyapatite" J.Mater. Sci., Vol: 31, pp. 1-21.
Neuman, W.F., Toribara, T.Y. and Mulryan, B.J., 1956, "Surface Chemistry of Bone (IX) Carbonate-Phosphate Exchange", J. Am. Chem. Soc., Vol. 78, pp. 4263-4266.
Poster A.S., Betts, F., and Blumenthal, N.C., 1980, "Formation and Structure of Synthetic and Bone Hydroxyapatites", Prog. Crystal Growth Charact., Vol. 3, pp. 49-64.
Ravaglioli, A. and Krajewski, A.,1992, "Bioceramics: Materials, Properties, Applications", Chapman & Hall, London, England, 1992, 422p.
Ressler, T., 1997, "WinXAS: A New Software Package not Only for the Analysis of Energy-Dispersive XAS Data", J. Physique, Vol. 7, No.C2, pp. 269-270.
Samachson, J. and Schmitz, A., 1969, "Slow Reactions of Calcium and Zinc Ions with the Surfaces of Bone Powder and Inorganic Bone", Biochim. Biophys. Acta, Vol. 192, pp. 231-237.
Silva, V.V. and Fernandes, R.Z.D., 1997, "Hydroxyapatite Ceramics from Powders Prepared by Precipitation Method", Aqueous Chemistry and Geochemistry of Oxides, Oxyhydroxides and Related Materials, pp. 189-194.
Silva V.V. and Domingues, R.Z., 1997, "Hydroxyapatite – Zirconia Composites Prepared by Precipitation Method", J. Mater. Sci. Mater. Med., Vol. 8, pp. 907-910.
Silva, V.V. and Lameiras, F.S., 2000, "Synthesis and Characterization of Composite Powders of Partially Stabilized Zirconia and Hydroxyapatite", Mater. Charact., Vol. 45, pp. 51-59.
Silva V.V., Lameiras, F.S. and Domingues, R.Z., 2001, "Microstructural and Mechanical Study of Zirconia-Hydroxyapatite (ZH) Composite Ceramics for Biomedical Applications", Comp. Sci. Tech., Vol. 61, pp. 301-310.
Silva, V.V., Lameiras, F.S. and Lobato, Z.I.P., 2002, "Biological Reactivity of Zirconia - Hydroxyapatite Composites", J. Biomed. Mater. Res. App. Biomat., Vol. 63, pp. 583-590.
Silva V.V., Lameiras, F.S. and Domingues, R.Z., 2003, "Processo de Obtenção de Compósitos de Zircônia Parcialmente Estabilizada com Cálcia - Hidroxiapatita (ZH), Aparelhagem, Produto e Usos", BRA Patent PI 0105243.
Stern, E.A., Siegel, R.W., Newville, M., Sanders, P.G. and Haskel, D., 1995, "Are Nanophase Grain Boundaries Anomalous?", Phys. Rev. Lett., Vol. 75, pp. 3874-3877.
Stevens, R., 1986, "Zirconia and Zirconia Ceramics", Magnesium Elektron Ltd, Twickenham, United Kingdom, 51p.
Takaqi, N., Mochida, M., Uchida, N., Saito, K. and Uematsu, K., 1992, "Filter Cake Forming and Hot Isostatic Pressing for TZP-Dispersed Hydroxyapatite Composite", J. Mater. Sci. Mater. Med., Vol. 3, pp. 199-203.
Tas, A.C., Korkusuz, F., Timucin, M. and Akkas, N., 1997, "An Investigation of the Chemical Synthesis and High –Temperature Sintering Behavior of Calcium Hydroxyapatite (HA) and Tricalcium Phosphate (TCP) Bioceramics", J. Mater. Sci. Mat. Med., Vol. 8, pp. 91-96.

7. Responsibility notice

The author(s) is (are) the only responsible for the printed material included in this paper.